

Correlation Analysis of Papillary Thyroid Carcinoma on Sonographic Features and Cervical Lymph Node Metastasis

Lihua Zhou

Zhejiang Chinese Medical University

Qiaodan Zhu

Zhejiang Chinese Medical University

Jincao Yao

Zhejiang Cancer Hospital

Di Ou

Zhejiang Cancer Hospital

Chen Yang

Zhejiang Cancer Hospital

Dong Xu (✉ xudong@zjcc.org.cn)

Zhejiang Cancer Hospital

Research

Keywords: Ultrasonography, Thyroid Cancer, Papillary, Lymphatic metastasis

Posted Date: May 14th, 2020

DOI: <https://doi.org/10.21203/rs.3.rs-28179/v1>

License:   This work is licensed under a Creative Commons Attribution 4.0 International License. [Read Full License](#)

Abstract

Background Papillary thyroid carcinoma (PTC) is the most common pathological type of thyroid carcinoma. We aim to evaluate the correlation between sonographic features of PTC and cervical lymph node metastasis (CLNM).

Methods A total of 1335 patients who underwent thyroidectomy and had pathologically confirmed unifocal PTC were enrolled in the retrospective research. Univariate analysis and logistic analysis were performed to predict CLNM by several independent variables. Receiver operating characteristic (ROC) curve was executed to evaluate the diagnostic performance.

Results Univariate analysis showed that location, aspect ratio, margin, echogenic foci, TI-RADS score and grade were related to CLNM ($P < 0.05$). Logistic analysis on sonographic features showed that margin and echogenic foci were independent correlative factors. Meanwhile, logistic analysis included clinical information, ultrasonic measurements and sonographic features showed that gender, age, tumour maximum diameter and volume, cross-sectional aspect ratio, location, margin and echogenic foci were independent correlative factors. The ROC curves were established based on the relevant factors, the AUC of tumour maximum diameter, tumour volume and margin were 0.738, 0.733, and 0.711, respectively. The regression model was constructed with AUC of 0.813, specificity of 70.3%, and sensitivity of 78.5%. ANOVA variance analysis on positive and negative group, tumour maximum diameter, margin, echogenic foci, TI-RADS score and grade had statistical significance ($P < 0.05$).

Conclusion Lower location, larger lesion, margin and echogenic foci were high risk factors for CLNM in PTC, cross-sectional aspect ratio ≥ 1 had more effective predictive value than longitudinal-sectional aspect ratio. Tumor volume was more effective to evaluate the lateral metastasis than maximum tumour diameter, it could guide preoperative FNA for CLNM.

Background

As a noninvasive imaging examination method, ultrasonography has been widely used in clinic, since the ultrasound images of the benign and malignant thyroid nodules overlap to some extent, TI-RADS regulates the classification diagnostic criteria, which has a better guidance in judgement of thyroid nodules. The TI-RADS white paper which was proposed by ACR in 2017 has been internationally recognized and used recently [1], it presented the characteristics of thyroid nodules based on sonographic features such as composition, echogenicity, shape, margin and echogenic foci.

PTC is the most common pathological type of thyroid carcinoma, among which unifocal tumour often occurs and the incidence of multifocal is about 30% [2]. CLNM is prone to occur early, and there is a risk of postoperative recurrence and distant metastasis [3]. However, there are many limitations in ultrasonography of cervical lymph nodes, especially central lymph nodes metastasis. Therefore, we study the correlative factors before surgery in order to predict the risk of lymph node metastasis, which is closely associated with treatment protocol and prognosis. In this study, unifocal PTC was selected to analyze in combination with clinical information, ultrasonic features and ACR ti-rads.

Materials And Methods

Patients

3570 patients were symptomatic with palpable or incidental thyroid lumps, and all of them finally underwent thyroidectomy in our hospital from July 2014 to September 2018 were enrolled. Inclusion criteria: 1. thyroidectomy

performed for the first time; 2. enhanced CT scan of neck and thorax to assess cervical lymph node and pulmonary metastasis, and ultrasonography performed for thyroid and neck before operation; 3. PTC was confirmed by biopsy before surgery. Exclusion criteria: 1. lung or other distant metastasis; 2. postoperative pathology diagnosed multifocal PTC. Finally, a total of 1335 patients with 1335 lesions were included in the study, their clinical data and ultrasonic images were retrospectively analyzed. There were 299 males and 1036 females, aged 12 to 84 years, with mean age 45.3 ± 11.8 years; the tumour maximum diameter was 3.5 to 64.7 mm, with an average diameter of 10.3 ± 7.9 mm. Unilateral thyroid lobe plus isthmus excision or total thyroidectomy were performed for the patients. If lateral lymph node metastasis were suspected by preoperative comprehensive evaluation, and confirmed by biopsy, lateral lymph node dissection would be performed [4-5]. All patients underwent preventive central lymph node dissection [4-6]. whether the dissected lymph node metastasized or not, metastatic lymph nodes were confirmed by pathology. This study was approved by the Ethics Committee of Cancer Hospital of the University of Chinese Academy of Sciences (Zhejiang Cancer Hospital), and all patients signed the informed consent form.

Machines

GE Logiq E9 ultrasonic instrument (General Electric Healthcare, Milwaukee) with a high-resolution linear probe (ML6-15) and Philips iU22 ultrasonic instrument (Philips Healthcare, Netherlands) with a high frequency linear probe (L12-5) were used for the examination.

Protocol

Patients were maintained at supine position with neck hyper-extended, then thyroid and double-sides neck were scanned at multi-section. The three diameters (length, width and depth), lesion location, composition, echogenicity, shape, margin and echogenic foci of the tumour were recorded and evaluated from workstations. The ultrasonic images were performed by two same professional physicians with experience of more than 10 years, both of them were board-certified physicians with training and experience of thyroid US. The ultrasonic images and reports were analyzed in a blind manner by two ultrasound specialists (with experience of more than 10 years) independently. All the imaging data were compared to the pathological results from neck dissections. In cases of discordance, the experienced sonologists (with experience of more than 20 years) in thyroid US reviewed the images and the final decision was determined.

Clinical information, ultrasonic measurements and features were used for data collection. Clinical information included gender, age; ultrasonic measurements included the tumour maximum diameter, tumour volume ($V=0.523 \times \text{length} \times \text{width} \times \text{depth}$), cross-sectional aspect ratio and longitudinal aspect ratio; ultrasonic features included ACR TI-RADS, Location1 represented left/right/isthmus, Location2 represented upper and lower (longitudinal scan)/anterior and posterior (longitudinal scan)/inside and outside (transversal scan) for each lobe.

The three diameters of the tumour were stated precisely as the following, we did a longitudinal scan of thyroid, selected the maximum section of the nodule, measured the maximum long diameter, it was length, then measured vertical diameter of long diameter, it was depth. Transversal scan of thyroid was executed, selected the maximum section of the nodule, measured the maximum diameter from left to right, it was width.

Cross-sectional aspect ratio=depth/width and longitudinal aspect ratio=depth/length.

Sonographic features according to ACR TI-RADS were carried out: composition (cystic, mixed cystic and solid, solid or almost completely solid), echogenicity (anechoic, hyperechoic or isoechoic, hypoechoic), shape (aspect ratio<1 or ≥1), margin (smooth or ill-defined/lobulated or irregular/extra-thyroid extension) and echogenic foci (none or large comet-tail artifacts/ macro/ peripheral / punctate echogenic foci).

Statistical analysis

The obtained data were statistically analyzed by SPSS 20.0 software. Data-counting were described statistically by the number of cases and rates. Chi-square test and independent-sample T test were used for univariate analysis. A multivariate analysis using binary logistic regression analysis should be adopted if analysis index $p < 0.05$ in the univariate analysis to further determine whether it was an independent correlative factor for CLNM. Logistic regression analysis fitting equation was used to predict the risk of CLNM. The receiver operating characteristic curve (ROC) area under the curve (AUC) was used to evaluate the prediction efficiency of the regression model. ANOVA variance analysis was used between positive and negative group. $P < 0.05$ was considered statistically significant.

Results

According to the inclusion and exclusion criteria, a total of 1335 patients were included in this study, there were 432 cases in positive group (32.4%), including 285 (21.4%) with only central lymph node metastasis, 54 (4.0%) with only lateral lymph node metastasis, and 93 (7.0%) with metastasis both in central and lateral lymph node), and there were 903 cases included in negative group (67.6%).

By comparing ultrasonic features of patients in positive and negative group, the results showed that location ($\chi^2=14.905$, $P=0.001$; $\chi^2=24.671$, $P=0.002$), aspect ratio ($\chi^2=23.421$, $P<0.001$), margin ($\chi^2=233.974$, $P<0.001$), echogenic foci ($\chi^2=146.635$, $P<0.001$), TI-RADS score ($t=-12.712$, $P<0.001$), and TI-RADS score ($\chi^2=177.050$, $P<0.001$) showed significant differences, while composition and echogenicity were not significant (Table 1, Figure 1-5 based on ACR TI-RADS).

Location, aspect ratio, margin and echogenic foci were included in the analysis. The results showed that margin (OR=2.195, 95% CI 1.927~2.501, $P<0.001$) and echogenic foci (OR=1.480, 95% CI 1.347~1.626, $P<0.001$) were independent correlative factors for CLNM (Table 2).

The clinical information, ultrasonic measurements and sonographic features were included in the analysis. The result showed that gender (OR=1.756, 95% CI 1.282~2.404, $P<0.001$), age (OR=0.958, 95% CI 0.947~0.970, $P<0.001$), maximum tumour diameter (OR=1.085, 95% CI 1.046~1.125, $P<0.001$), tumour volume (OR=0.926, 95% CI 0.863~0.995, $P=0.035$), cross-sectional aspect ratio (OR=2.202, 95% CI 1.054~4.599, $P=0.036$), location2 (OR=1.068, 95% CI 1.010~1.130, $P=0.022$), margin (OR=2.044, 95% CI 1.764~2.369, $P<0.001$) and echogenic foci (OR=1.268, 95% CI 1.139~1.413, $P<0.001$) were independent risk factors for CLNM (Table 3).

Logistic regression analysis was used to obtain the independent correlative factors for CLNM. Gender, age, maximum tumour diameter and volume, cross-sectional aspect ratio, location2, margin and echogenic foci were analyzed by the ROC curve. The AUC, specificity, sensitivity of maximum tumour diameter was 0.738, 66.6%, and 69.9%, respectively. For tumour volume, the AUC, specificity and sensitivity were 0.733, 67.6%, and 68.1%, respectively. For margin, the AUC, specificity and sensitivity were 0.711, 81.1%, and 60.4%, respectively. To take CLNM in PTC patients as a dependent variable, gender, age, maximum tumour diameter and volume, cross-sectional aspect ratio, location2, margin and echogenic foci as covariates, a regression equation of CLNM was deduced from the parameters, $Y = -2.521 + 0.563 \times X_1 - 0.042 \times X_2 + 0.081 \times X_3 - 0.076 \times X_4 + 0.789 \times X_5 + 0.066 \times X_6 + 0.715 \times X_7 + 0.238 \times X_8$ (Y represented as CLNM, X_1 =gender, X_2 =age, X_3 =maximum tumour diameter, X_4 =tumour volume, X_5 =cross-sectional aspect ratio, X_6 =location2, X_7 =margin, X_8 =echogenic foci). The ROC curve was used to evaluate the regression model constructed by combining five independent correlative factors, in which the value of AUC, specificity and sensitivity was 0.813, 70.3% and 78.5%, respectively (Figure 6).

According to the differences in clinical information, ultrasonic measurements and features by ANOVA variance analysis, six pair-to-pair comparison groups were divided into only central metastasis group, only lateral metastasis group, both metastatic group and negative group. The results showed that significant variables ($P < 0.05$) among five groups included tumour maximum diameter, margin, echogenic foci, ti-rads score and grade; among four groups was tumour volume; between three groups was aspect ratio; between two groups were gender, age and cross-sectional aspect ratio; between one group was location2. For location1, there was no significant difference. The comparison between six pair-to-pair groups was shown in table 4.

Discussion

With the application of high frequency ultrasound, the incidence of thyroid lesions in adults can be up to 60~70% [7]. FNA has been the most effective diagnostic method for benign and malignant thyroid neoplasms recently [8]. However, regular observation is one of the choices for most benign nodules, even malignant nodules, especially malignant nodules <1cm or selected patients with contraindications for surgical procedure [9-10]. Therefore, the standardization of thyroid ultrasound images by ti-rads can effectively improve the differential diagnosis of thyroid nodules.

PTC is the most common malignant thyroid tumour, lymph node metastasis of which were associated with the diameter, location, number and invasive growth of primary tumour [11-12]. As the preferred examination method for thyroid, ultrasonography has the detection rate of 18.8%-31% only in that the interference from trachea, esophagus, osseous tissue and thyroid underlying diseases limits the detection of cervical lymph nodes [13-14]. Meanwhile, TI-RADS was mainly adopted in the differential diagnosis of benign and malignant thyroid neoplasms. The consistent conclusion of the correlation between gender, age and sonographic features and lymph node metastasis was difficult to achieve [15-17]. This study only included unifocal PTC and conducted a stratified study to comprehensively evaluate the risks of CLNM in PTC combined with clinical information, ultrasonic measurements and TI-RADS to obtain a more complete and effective result.

PTC can occur in any part of thyroid, including bilateral lobes and isthmus. For isthmus, the incidence of thyroid cancer is about 2.5%~9.2% [18]. Studies have found that isthmus PTC was more likely to invade thyroid capsule and surrounding tissues, compared with the lateral lobe PTC [18-19]. This is mainly because when the tumour grows to some extent, the area of the isthmus tumour in contact with thyroid capsule is relatively large, which is easy to invade the capsule or break through the capsule and invade the surrounding tissues, thus CLNM would happen. Previous studies [20-21] have suggested that when the tumour was located in the middle or lower pole of thyroid, the risk of CLNM was increased. In this study, 29.9% (177/591) and 32.2% (213/662) of lymph node metastasis occurred in the left and right lobes, respectively, while the incidence of PTC lymph node metastasis in isthmus was 51.2% (42/82), and the lobes were stereolocated by the upper and lower, anterior and posterior, inside and outside, 43.8% (28/64) of lymph node metastasis occurred in the lower, anterior and outside location, which were consistent with previous studies. location showed significant difference in univariate analysis only and Logistic regression analysis just showed statistical significance in location2. However, more data should be provided to promote and confirm the result.

Aspect ratio ≥ 1 is a highly specific index for the diagnosis of malignant thyroid nodules [22-23]. According to previous literature, the results of correlation between aspect ratio and CLNM in PTC were not consistent. Part of literature [24-25] suggested that it was prone to occur CLNM when aspect ratio >1 , and CLNM was the risk factor. Some study [26] reported that no statistical significance could be seen in the prediction of lateral cervical lymph node metastasis in the case of aspect ratio ≥ 1 . In this study, aspect ratio had statistical significance in univariate analysis while had no significance in multivariate analysis. 432 cases occurred CLNM, and 44.2% (191/432) were PTMC. 66% (126/191) of PTMC patients with CLNM had aspect ratio ≥ 1 , 38.2% (92/241) of PTC patients with CLNM has aspect ratio ≥ 1 , it meant that aspect ratio ≥ 1 was of greater significance for PTMC.

In addition, according to the morphology of the thyroid lesion, it could be divided into cross-sectional aspect ratio and longitudinal section aspect ratio, among which 45.8% (198/432) of the patients with CLNM had cross-sectional aspect ratio ≥ 1 , and 28.9% (125/432) had longitudinal section aspect ratio ≥ 1 . We concluded that cross-sectional aspect ratio had a better predictive value for CLNM in PTC, compared with the longitudinal aspect ratio. This need to be further confirmed by subsequent study.

The incidence of lymph node metastasis is increased with the growth of malignant tumour accompanied by the invasion and expansion of cancer cells [27-28]. Margin is one of the invasive characteristics of the tumour. The nodules with high invasiveness showed irregular and lobulated boundaries, while smooth boundaries generally indicate low invasiveness and slow growth [29]. In this study, out of the patients with ti-rads score of 0 (smooth or ill-defined), 18.9% (171/903) of the patients had CLNM, while 60.4% (261/432) of the patients with lobular/irregular or extension had CLNM. Univariate analysis and logistic regression analysis both showed a good correlation between margin and CLNM in PTC.

Echogenic foci are divided into micro-calcification, macro-calcification and ring calcification around the nodules on the basis of 1mm [30]. Micro-calcification can reflect the psammoma bodies in pathology, which results from calcification and necrosis of cancer cells and is a specific indicator for the diagnosis of PTC [31], and it is significantly related to

lymph node metastasis. Continuous follow-up studies found that CLNM was more likely to occur in PTC with micro-calcification [32]. In this study, among the cases with ti-rads score of 0 (none or large comet-tail artifacts), 20.7% (174/838) of the patients had CLNM, while 53.4% (250/468) of the patients with peripheral calcification or punctate echogenic foci had CLNM. Therefore, ultrasonography can better predict the risk of CLNM in PTC for the different types of calcifications.

Ti-rads comprehensively evaluated the tumour according to sonographic features of thyroid nodules, such as composition, echogenicity, aspect ratio, margin, echogenic foci. Its scoring and grading system were used for the differential diagnosis of benign and malignant nodules, it would be great value for further determination of diagnosis and treatment protocols. In this study, ti-rads score of positive group (7.46 ± 2.075) was significantly higher than that of negative group (6.03 ± 1.838), but 13.0% (173/1335) of the cases were confirmed TR3, it meant TI-RADS of benign and malignant nodules overlapped to some extent. Only by combining ti-rads with clinical information and ultrasonic measurements, it can achieve the better diagnosis of CLNM in PTC. In this study, gender, age, ultrasonic measurements and features were included for logistic regression analysis to establish a prediction model for CLNM, with a specificity of 70.3% and a sensitivity of 78.5%.

CLNM in PTC generally first occurs in the central region and then to the lateral region [33], which is more common in area VI, followed by area III and IV [34]. However, not all PTC lymph node metastases follow this pattern, with some skip metastasis where lymph node metastasis occurs in the lateral neck region and no metastasis in the ipsilateral central region [35]. Some studies have reported that the rate of lymph node skip metastasis was 3~21.8%[36]. Due to only unifocal PTC included in this study, the lymph node skip metastasis rate was 4.0%.

In this study, six pair-to-pair comparison groups including only central metastasis group, only lateral metastasis group, both metastatic group and negative group were classified using ANOVA variance analysis, and maximum tumour diameter, margin, echogenic foci, TI-RADS score and grade in 5 groups (except lateral group and both metastasis group) had statistical significance ($P<0.05$). 432 cases occurred CLNM, among which 66% (285/432) were in only central metastasis group, the average tumour volume is 1.12ml; 34% (147/432) were in lateral metastasis, including only lateral and both metastatic groups, the average tumour volume is 3.89ml. For maximum tumour diameter, the average sizes of these groups were 11.7mm and 19.6mm, respectively. It indicated that tumor volume could be more effective to evaluate the different metastasis region than maximum tumour diameter, but further refinement of metastatic lymph nodes is required.

This article was a retrospective analysis. Cases of unifocal PTC and lymph node dissection performed in the central area of the neck were merely included in this study, which may cause selection bias. In addition, cases with metastases in lateral location, and cases with both central and lateral location were not adequate, therefore, large samples are required to study the cervical metastases in different parts.

Conclusion

In conclusion, ti-rads for the evaluation of CLNM in PTC has a good reference value for preoperative evaluation of the risk of lymph node metastasis. When PTC has CLNM, the location, margin and echogenic foci of the tumour have certain particularity. For PTC patients with lower location, large tumour, cross-sectional aspect ratio ≥ 1 , lobulated or irregular margin, peripheral calcification or punctate echogenic foci as high-risk factors, related examination for cervical lymph node should be conducted in details, such as cervical lymph node sonographic scan by the experienced sonologists (with experience of more than 10 years) and enhanced CT scan of neck as a rule, then the accuracy of cervical metastatic lymph nodes examination will be improved.

Abbreviations

PTC Papillary thyroid carcinoma

CLNM Cervical lymph node metastasis

TI-RADS Thyroid imaging report and data system

FNA Fine-needle aspiration

ACR American College of Radiology

ROC Receiver operating characteristic

AUC Area under the curve

OR Odds ratio

CI Confidence interval

PTMC Papillary thyroid microcarcinoma

Declarations

Ethics approval and consent to participate:

This study was approved by the Ethics Committee of Cancer Hospital of the University of Chinese Academy of Sciences (Zhejiang Cancer Hospital).

Consent for publication:

Informed consent was obtained from all patients in this study. The scientific guarantor of this publication is Prof. Dong Xu, and consent for publication is acquired from all authors.

Availability of data and material:

All authors promise data and material are available and reliable. Prof. Dong Xu provided statistical advice for this manuscript. No complex statistical methods were necessary for this paper.

Competing interests:

The authors of this manuscript declare no relationships with any companies, whose products or services may be related to the subject matter of the article.

Funding:

This work was supported by National Natural Science Foundation of China (NO. 81871370) and Zhejiang Provincial Natural Science Foundation of China (NO. LSD19H180001).

Authors' contributions:

Lihua Zhou and Jincao Yao contributed equally to this work.

Dong Xu and Chen Yang are corresponding authors for this article.

Acknowledgements:

Not applicable.

References

- [1] Franklin NT, Willian D, Edward GG, et al. ACR thyroid imaging, reporting and data system (TI-RADS): white paper of the ACR TI-RADS committee[J]. J Am Coll Radiol, 2017, 14:587-595.
- [2] Lim H, Devesa SS, Sosa JA, et al. Trends in thyroid cancer incidence and mortality in the united states, 1974-2013[J]. JAMA, 2017, 317(13):1338-1348. DOI:10.1001/jama.2017.2719.
- [3] Kim SY, Kwak JY, Kim EK, et al. Association of preoperative US features and recurrence in patients with classic papillary thyroid carcinoma[J]. Radiology, 2015, 277(2):574-583. DOI:10.1148/radiol.2015142470.
- [4] Chinese Association of Thyroid Oncology (CATO). Chinese experts' consensus on diagnosis and treatment of thyroid micropapillary carcinoma (2016 Edition). Chin J Clin Oncol, 2016, 43(10):405-411.

- [5] Chinese Thyroid Association (CTA), Thyroid Committee of Chinese Research Hospital Association. Expert consensus on lymph node dissection in cervical region of differentiated thyroid cancer (2017Edition)[J]. *Chin J Practical Surg*, 2017, 37(9):985-991.
- [6] Wang TS, Evans DB. Commentary on: Occult lymph node metastasis and risk of regional recurrence in papillary thyroid cancer after bilateral prophylactic central neck dissection: A multi-institutional study[J]. *Surgery*, 2017, 161(2):472-474.
- [7] Guth S, Theune U, Aberle J, et al. Very high prevalence of thyroid nodules detected by high frequency (13MHz) ultrasound examination. *Eur J Clin Invest*, 2009, 39:699-706.
- [8] Singh Ospina N, Brito JP, Maraka S, et al. Diagnostic accuracy of ultrasound-guided fine needle aspiration biopsy for thyroid malignancy: systematic review and meta-analysis. *Endocrine*, 2016, 53:651-661.
- [9] Simth-Bindman R, Lebda P, Feldstein VA, et al. Risk of thyroid cancer based on thyroid ultrasound imaging characteristics: results of a population-based study. *JAMA Intern Med*, 2013, 173:1788-1796.
- [10] Davies L, Welch HG. Current thyroid cancer trends in the United States. *JAMA Otolaryngol Head Neck Surg*, 2014, 140:317-322.
- [11] Haugen BR, Alexander EK, Bible KC, et al. 2015 American Thyroid Association Management Guidelines for Adult Patients with Thyroid Nodules and Differentiated Thyroid Cancer: The American Thyroid Association Guidelines Task Force on Thyroid Nodules and Differentiated Thyroid Cancer[J], 2016, 26(1):1-133. DOI:10.1089/thy.2015.0020.
- [12] Park JP, Roh JL, Lee JH, et al. Risk factors for central neck lymph node metastasis of clinically noninvasive, node-negative papillary thyroid microcarcinoma[J]. *Am J Surg*, 2014, 208(3):412-418. DOI:10.1016/j.amjsurg.2013.10.032.
- [13] Li JW, Chang C, Chen M, et al. Identification of calcifications in thyroid nodules: comparison between ultrasonography and CT[J]. *Chin J Ultrasonogr*, 2017, 26(5):313-317.
DOI:10.3760/cma.j.issn.1004-4477.2017.05.012.
- [14] Zhu Q, Li JW, Zhou SC, et al. Diagnostic value of ultrasonography in predicting neck lymph node metastasis in Hashimoto's thyroiditis with papillary thyroid carcinoma[J]. *Chin J Ultrasonogr*, 2016, 25(11):962-965.
DOI:10.3760/cma.j.issn.1004-4477.2016.11.011.
- [15] AL AA, Williams BA, Rigby MH, et al. Multifocal papillary thyroid cancer increases the risk of central lymph node metastasis[J]. *Thyroid*, 2015, 25(9):1008-1012. DOI:10.1089/thy.2015.0130.
- [16] Lin DZ, Qu N, Shi RL, et al. Risk prediction and clinical model building for lymph node metastasis in papillary thyroid microcarcinoma[J]. *Onco Targets Ther*, 2016, 9:5307-5316. DOI:10.2147/OTT.S107913.
- [17] Qu N, Zhang L, Lin DZ, et al. The impact of coexistent Hashimoto's thyroiditis on lymph node metastasis and prognosis in papillary thyroid microcarcinoma[J]. *Tumour Biol*, 2016, 37(6):7685-7692. DOI:10.1007/s13277-015-4534-4.
- [18] Lee YS, Jeong JJ, Nam KH, et al. Papillary carcinoma located in the thyroid isthmus[J]. *World J Surg*, 2010, 34(1):36-39.

- [19] Fan FJ, Qin L, Ding HY, et al. Study on ultrasound image features of papillary thyroid carcinoma originating in the isthmus [J]. *Chin J Clinicians (Electronic Edition)*, 2015, 9(20): 3720-3723.
- [20] Xiang D, Xie L, Xu Y, et al. Papillary thyroid microcarcinomas located at the middle part of the middle third of the thyroid gland correlates with the presence of neck metastasis[J]. *Surgery*, 2015, 157(3):526-533. DOI:10.1016/j.surg.2014.10.020.
- [21] Sun W, Lan X, Zhang H, et al. Risk factors for central lymph node metastasis in CNO papillary thyroid carcinoma: a systematic review and meta-analysis[J]. *PLoS One*, 2015, 10(10): e0139021. DOI:10.1371/journal.pone.0139021.
- [22] Kwak JY, Han KH, Yoon JH, et al. Thyroid imaging reporting and data system for US features of nodules: a step in establishing better stratification of cancer risk. *Radiology*, 2011, 260:892-899.
- [23] Na DG, Baek JH, Sung JY, et al. Thyroid imaging reporting and data system risk stratification of thyroid nodules: categorization based on solidity and echogenicity. *Thyroid*, 2016, 26:562-572.
- [24] Nam SY, Shin JH, Han BK, et al. Preoperative ultrasonographic features of papillary thyroid carcinoma predict biological behavior[J]. *J Clin Endocrinol Metab*, 2013, 98(4):1476-1482.
- [25] Zhou J, Zhou SC, Li JW, et al. Risk factors of central neck lymph node metastasis following solitary papillary thyroid carcinoma[J]. *Chin J Ultrasonogr*, 2019, 28(3):235-240.
- [26] Deng SP, Xiong HH, Li QS, et al. Ultrasonographic characteristics of papillary thyroid cancer: predicting factors of lateral lymph node metastasis[J]. *Chinese J Ultrasound Med*, 2017, 33(3):196-198.
- [27] Heaton CM, Chang JL, Orloff LA. Prognostic implications of lymph node yield in central and lateral neck dissections for well-differentiated papillary thyroid carcinoma[J]. *Thyroid*, 2016, 26(3):434-440.
- [28] Lan Y, Song Q, Jin Z, et al. Correction of routine ultrasound features and BRAFV600E gene to the cervical lymph node metastasis of thyroid papillary carcinoma[J]. *Med J Chin PLA*, 2019, 44(9):747-752.
- [29] Deng SP, Li QS, Chen SH, et al. Analysis of related factors on cervical lymph node metastasis and ultrasonographic characteristics of papillary thyroid microcarcinoma[J]. *J Clin Ultrasound in Med*, 2017, 19(6):424-426.
- [30] Oh EM, Chung YS, Song WY, et al. The pattern and significance of the calcifications of papillary thyroid microcarcinoma presented in preoperative neck ultrasonography[J]. *Ann Surg Treat Res*, 2014, 86(3):115-121.
- [31] Shi C, Li S, Shi T, et al. Correlation between thyroid nodule calcification morphology on ultrasound and thyroid carcinoma[J]. *J Int Med Res*, 2012, 40(1):350-357.
- [32] Bai Y, Zhou G, Nakamura M, et al. Survival impact of psammoma body, stromal calcification and bone formation in papillary thyroid carcinoma[J]. *Mod Pathol*, 2009, 22(7):887-894.
- [33] Zeng RC, Zhang W, Gao EL, et al. Number of central lymph node metastasis for predicting lateral lymph node metastasis in papillary thyroid microcarcinoma[J]. *Head Neck*, 2014, 36(1):101-106.
- [34] Kim KE, Kim EK, Yoon JH, et al. Preoperative prediction of central lymph node metastasis in thyroid papillary microcarcinoma using clinicopathologic and sonographic features[J]. *World J Surg*, 2013, 37(2):385-391.

[35] Lee YS, Shin SC, Lim YS, et al. Tumour location-dependent skip lateral cervical lymph node metastasis in papillary thyroid cancer[J]. *Head Neck*, 2014, 36(6):887-891. DOI: 10.1002/hed.23391.

[36] Lei JY, Zhong JJ, Jiang K, et al. Skip lateral lymph node metastasis leaping over the central neck compartment in papillary thyroid carcinoma[J]. *Oncotarget*, 2017, 8(16): 27022-27033. DOI:10.18632/oncotarget.15388.

Tables

Variable	Positive group n=432	Negative group n=903	Statistics	P
Location1 (left/right/isthmus)	177/213/42	414/449/40	$\chi^2=14.905$	P=0.001
Location 2 (upper anterior inside/upper posterior inside/upper posterior outside /lower anterior inside/lower anterior outside/lower posterior inside/ lower posterior outside/isthmus)	119/101/42/28/ 23/28/23/26/42	283/185/119/59/62/36/61/58/40	$\chi^2=24.671$	P=0.002
Composition (mixed cystic and solid/solid or almost completely solid)	10/422	10/893	$\chi^2=2.877$	P=0.089
Echogenicity (hyperechoic or isoechoic /hypoechoic)	424/8	894/9	$\chi^2=1.700$	P=0.192
Aspect ratio (<1/≥1)	214/218	322/581	$\chi^2=23.421$	P<0.001
Margin (smooth or ill-defined/lobulated or irregular/extra-thyroid extension)	171/229/32	732/160/11	$\chi^2=233.974$	P<0.001
Echogenic foci (none or large comet-tail artifacts/ macro/peripheral / punctate echogenic foci)	174/8/38/212	664/21/32/186	$\chi^2=146.635$	P<0.001
TI-RADS score	7.46±2.075	6.03±1.838	t=-12.712	P<0.001
TI-RADS grade (TR3/TR4/TR5)	23/146/263	150/537/216	$\chi^2=177.050$	P<0.001

Table 1 Correlation analysis of cervical lymph node metastasis in PTC

Variable	OR	95%CI	P
Location1(left/right/ isthmus)	1.161	0.920~1.466	P=0.209
Location 2	1.044	0.989~1.101	P=0.116
Aspect ratio	1.030	0.939~1.129	P=0.533
Margin	2.195	1.927~2.501	P<0.001
Echogenic foci	1.480	1.347~1.626	P<0.001

Table 2 Logistic regression analysis of CLNM in sonographic features

Variable	OR	95%CI	P
Gender (male/female)	1.756	1.282~2.404	P<0.001
Age	0.958	0.947~0.970	P<0.001
Maximum tumour diameter	1.085	1.046~1.125	P<0.001
Tumour volume	0.926	0.863~0.995	P=0.035
Cross-sectional aspect ratio	2.202	1.054~4.599	P=0.036
Location1(left/right/ isthmus)	1.156	0.907~1.474	P=0.242
Location 2 [upper and lower/ anterior and posterior/ inside and outside]	1.068	1.010~1.130	P=0.022
Aspect ratio	1.022	0.892~1.170	P=0.757
Margin	2.044	1.764~2.369	P<0.001
Echogenic foci	1.268	1.139~1.413	P<0.001

Table 3 Logistic regression analysis of CLNM in PTC

Variable	Central v.s. negative	Lateral v.s. negative	Both v.s. negative	Central v.s. lateral	Central v.s. both	Lateral v.s. both
Gender	P=0.021 ^a	P=0.674	P=0.011 ^a	P=1.000	P=0.677	P=0.912
Age	P<0.001 ^a	P=0.413	P<0.001 ^a	P=0.725	P=0.743	P=0.272
Maximum tumour diameter	P<0.001 ^a	P<0.001 ^a	P<0.001 ^a	P=0.002 ^a	P<0.001 ^a	P=0.270
Tumour volume	P=0.012 ^a	P=0.025 ^a	P<0.001 ^a	P=0.121	P<0.001 ^a	P=0.987
Cross-sectional aspect ratio	P=0.722	P=0.087	P<0.001 ^a	P=0.431	P<0.001 ^a	P=0.768
Location 1	P=0.079	P=0.924	P=0.612	P=1.000	P=1.000	P=1.000
Location 2	P=0.031 ^a	P=0.997	P=0.977	P=0.951	P=0.109	P=0.945
Aspect ratio	P=0.064	P=0.017 ^a	P<0.001 ^a	P=0.389	P=0.025 ^a	P=0.998
Margin	P<0.001 ^a	P<0.001 ^a	P<0.001 ^a	P<0.001 ^a	P<0.001 ^a	P=1.000
Echogenic foci	P<0.001 ^a	P<0.001 ^a	P<0.001 ^a	P<0.001 ^a	P<0.001 ^a	P=1.000
TI-RADS-score	P<0.001 ^a	P<0.001 ^a	P<0.001 ^a	P=0.005 ^a	P=0.004 ^a	P=1.000
TI-RADS-grade	P<0.001 ^a	P<0.001 ^a	P<0.001 ^a	P<0.001 ^a	P=0.002 ^a	P=0.571

Table 4 ANOVA variance analysis of CLNM in PTC

^a represented P<0.05

Figures

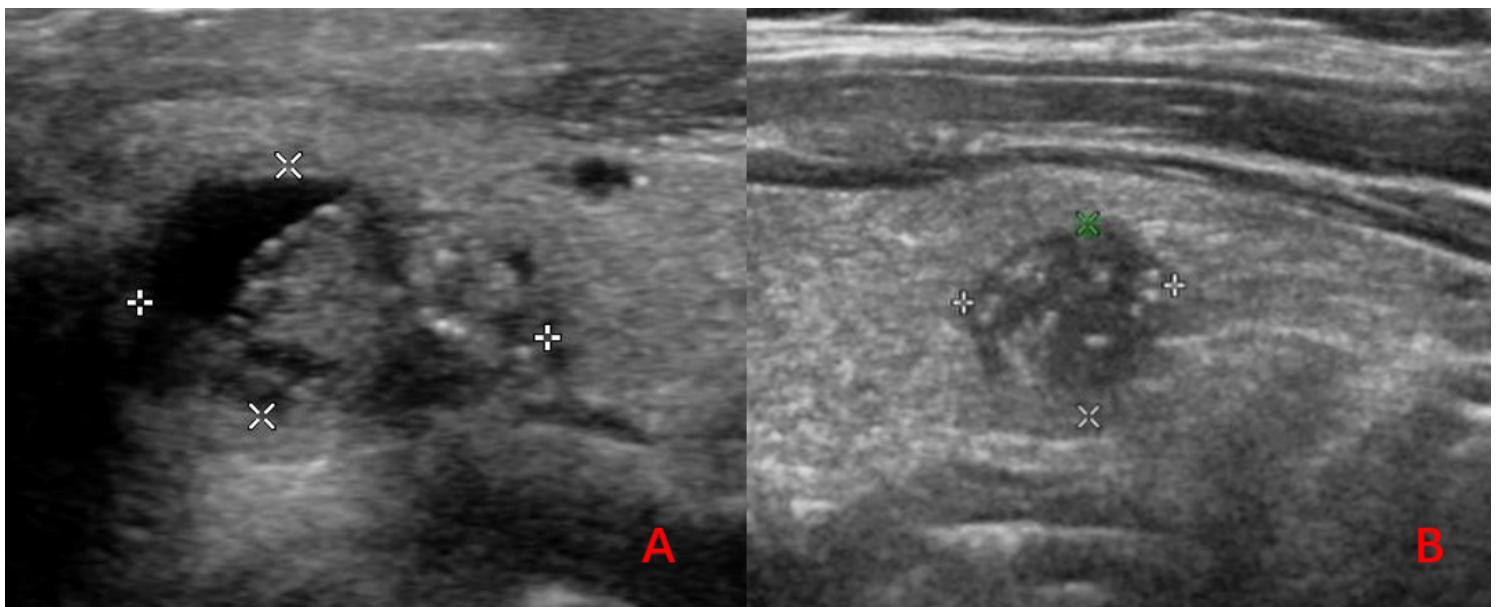


Figure 1

Legends not available in this version

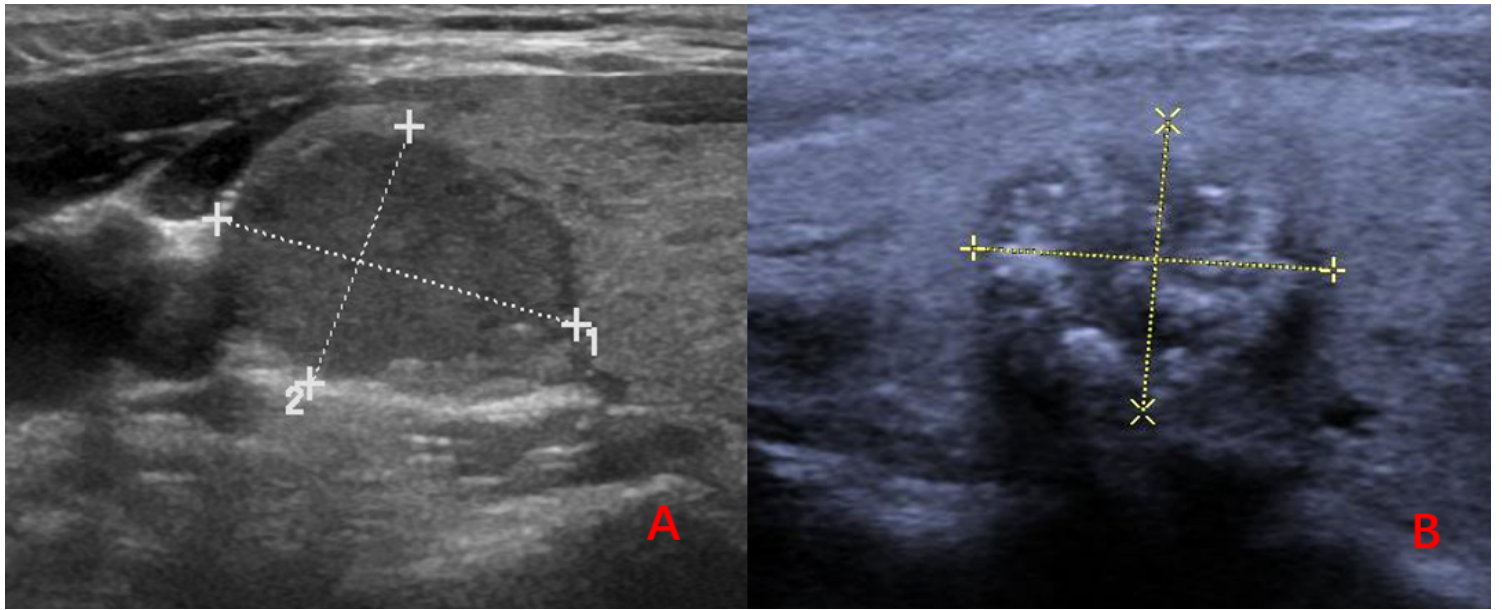


Figure 2

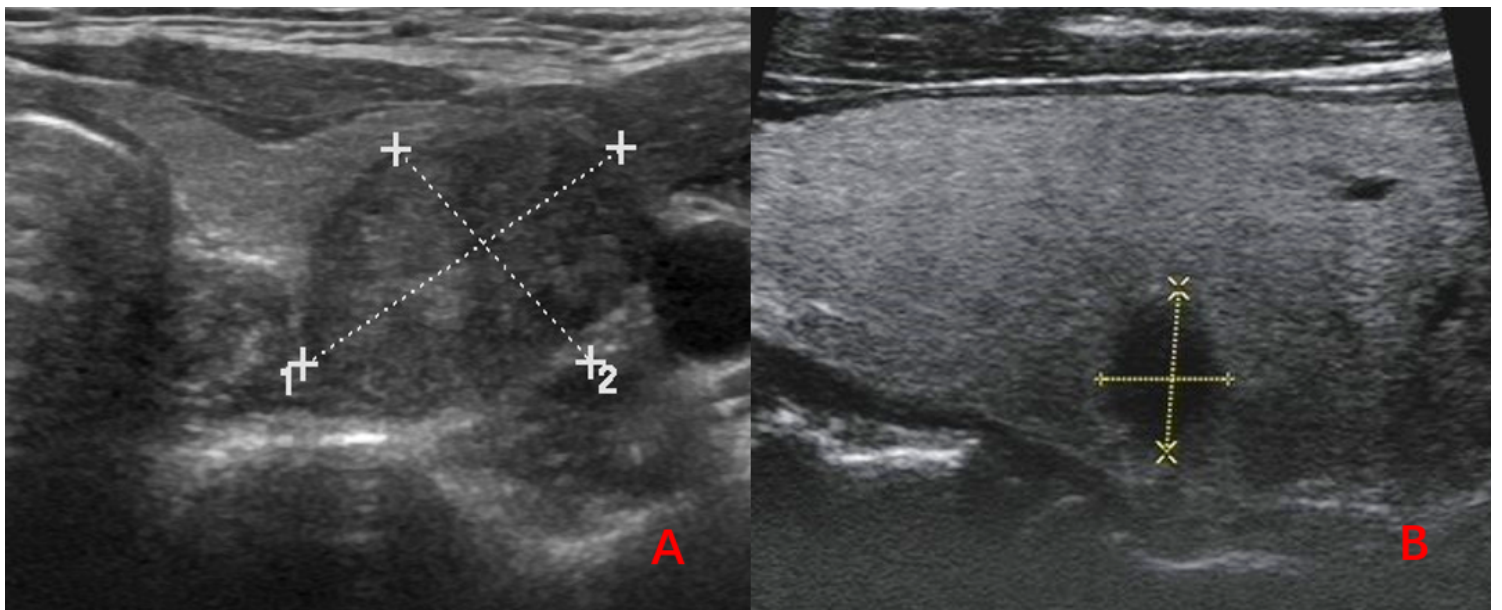


Figure 3

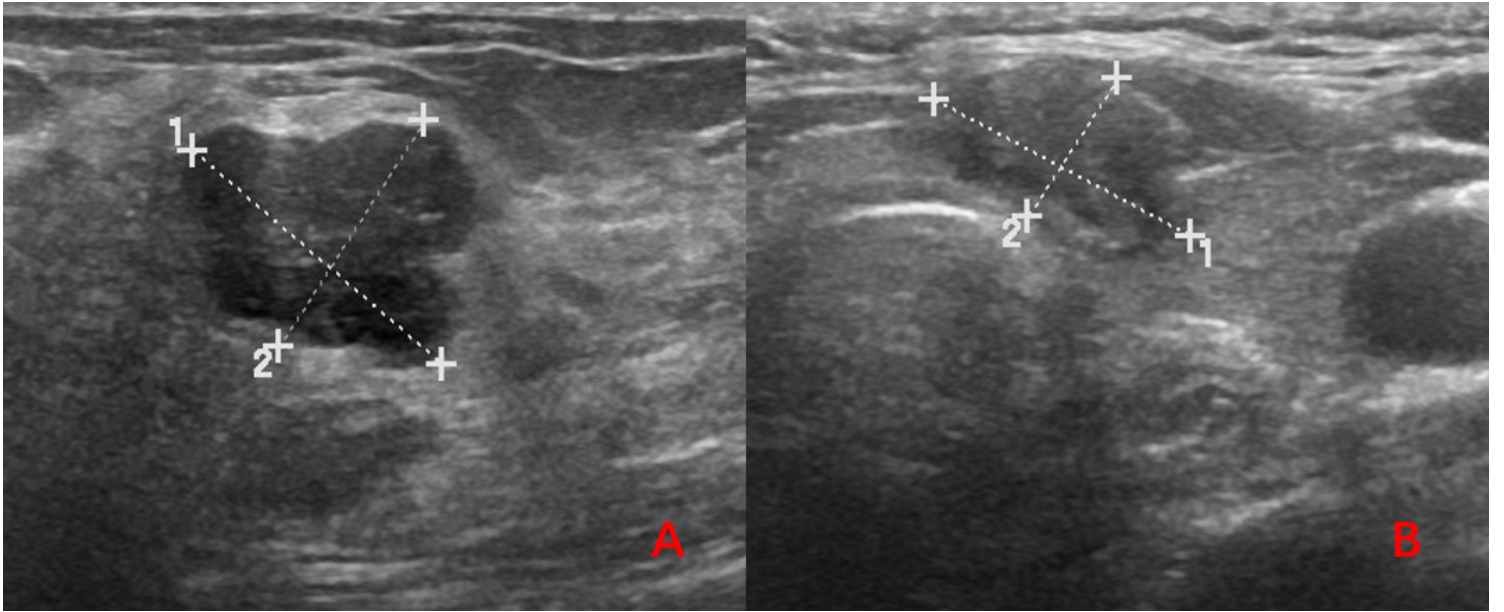


Figure 4

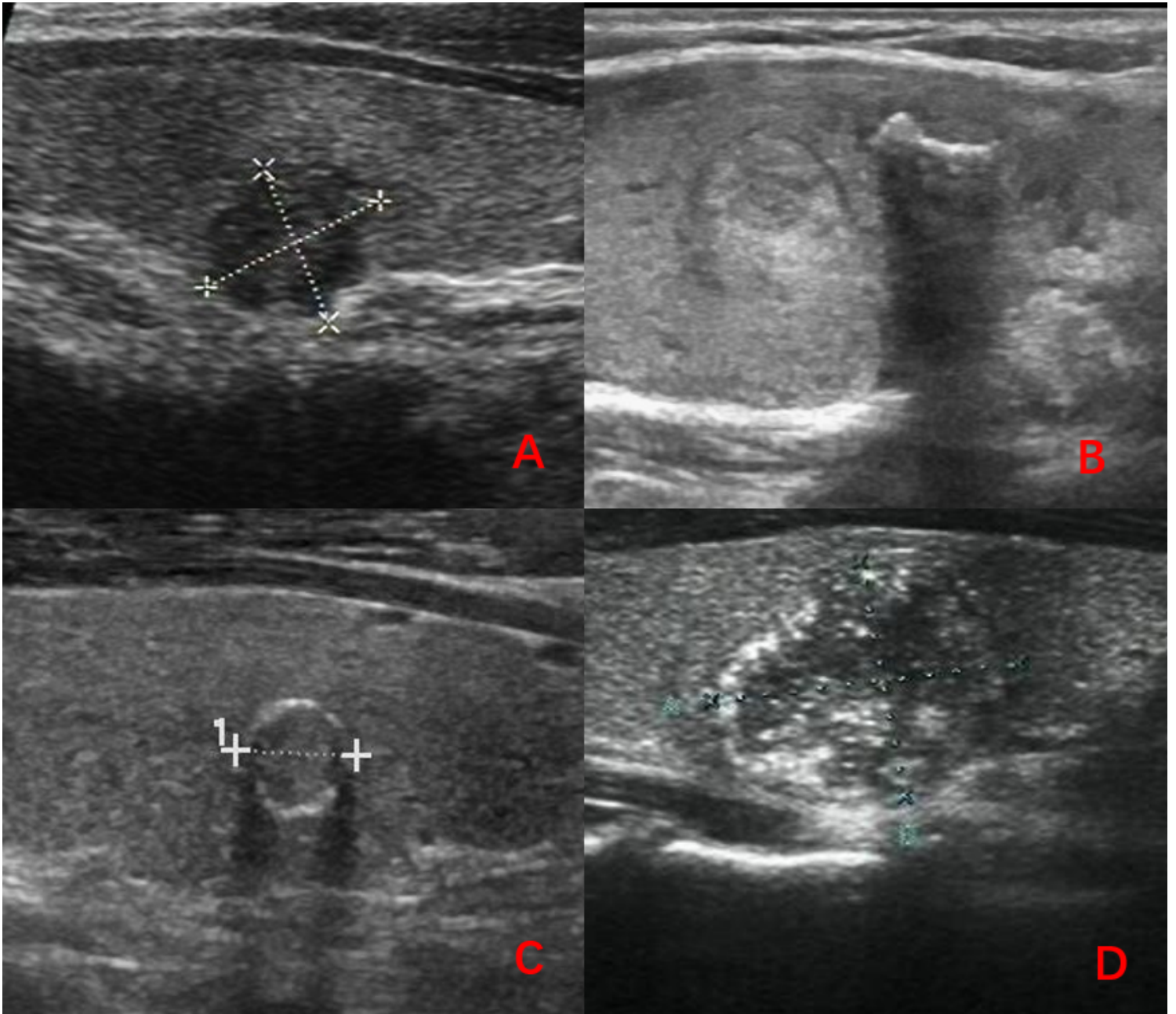


Figure 5

Supplementary Files

This is a list of supplementary files associated with this preprint. Click to download.

- [ROC.png](#)
- [PTCsonographicfeaturesandCLNM.pdf](#)
- [ROC.png](#)
- [PTCsonographicfeaturesandCLNM.pdf](#)